



American Society of Hematology  
 2021 L Street NW, Suite 900,  
 Washington, DC 20036  
 Phone: 202-776-0544 | Fax 202-776-0545  
 editorial@hematology.org

## Loss of stress sensor GADD45A promotes stem cell activity and ferroptosis resistance in LGR4/HOXA9-dependent AML

Tracking no: BLD-2024-024072R2

Nunki Hassan (University of Sydney, Australia) Hangyu Yi (University of Sydney, Australia) Bilal Malik (University of Sydney, Australia) Lucie Gaspard-Boulin (University of Sydney, Australia) Saumya E. Samaraweera (University of South Australia and SA Pathology, Australia) Debora Casolari (University of South Australia and SA Pathology, Australia) Janith Seneviratne (Children's Cancer Institute, Australia) Anushree Balachandran (Children's Cancer Institute, Australia) Tracy Chew (University of Sydney, Australia) Alastair Duly (Children's Cancer Institute, Australia) Daniel R. Carter (Children's Cancer Institute, Australia) Belamy Cheung (Children's Cancer Institute, Australia) Murray Norris (Children's Cancer Institute, Australia) Michelle Haber (Children's Cancer Institute, Australia) Maria Kavallaris (Children's Cancer Institute, Australia) Glenn M. Marshall (Children's Cancer Institute, Australia) Xu Dong Zhang (The University of Newcastle, Australia) Tao Liu (Children's Cancer Institute, Australia) Jianlong Wang (Columbia University Irving Medical Center, United States) Dan A. Liebermann (Temple University School of Medicine, United States) Richard J. D'Andrea (University of South Australia, Australia) Jenny Y. Wang (University of Sydney, Australia)

### Abstract:

The overall prognosis of acute myeloid leukemia (AML) remains dismal, largely due to the inability of current therapies to kill leukemia stem cells (LSCs) with intrinsic resistance. Loss of the stress sensor GADD45A is implicated in poor clinical outcomes but its role in LSCs and AML pathogenesis is unknown. Here we define GADD45A as a key downstream target of LGR4 oncogenic signaling and discover a regulatory role for GADD45A loss in promoting leukemia-initiating activity and oxidative resistance in LGR4/HOXA9-dependent AML, a poor prognosis subset of leukemia. Knockout of GADD45A enhances AML progression in murine and patient-derived xenograft (PDX) mouse models. Deletion of GADD45A induces substantial mutations, increases LSC self-renewal and stemness in vivo and reduces levels of reactive oxygen species (ROS), accompanied by decreased response to ROS-associated genotoxic agents (e.g., ferroptosis inducer RSL3) and acquisition of an increasingly aggressive phenotype upon serial transplantation in mice. Our single-cell CITE-seq analysis on patient-derived LSCs in PDX mice and subsequent functional studies in murine LSCs and primary AML patient cells show that loss of GADD45A is associated with resistance to ferroptosis (an iron-dependent oxidative cell death caused by ROS accumulation) through aberrant activation of antioxidant pathways related to iron and ROS detoxification such as FTH1 and PRDX1, upregulation of which correlates with unfavorable outcomes in AML patients. These results reveal a therapy resistance mechanism contributing to poor prognosis and support a role for GADD45A loss as a critical step for leukemia-initiating activity and as a target to overcome resistance in aggressive leukemia.

**Conflict of interest:** No COI declared

**COI notes:**

**Preprint server:** No;

**Author contributions and disclosures:** N.H. and B.M. performed drug treatment and ferroptosis-related experiments with input from X.D.Z., T.L. and J.W.; H.Y. performed murine model experiments; J.S., A.B., N.H. carried out single-cell experiments with input from D.R.C.; L.G. analyzed CITE-seq data with assistance from J.S. and T.C; A.D. performed in vivo bioluminescence imaging; S.E.S., D.A.C., R.J.D., D.A.L. supplied mouse Gadd45a<sup>-/-</sup> BM cells and provided input on murine model experiments; R.J.D., D.A.L., S.E.S., D.A.C., J.W., G.M.M., M.N., M.H., M.K., B.B.C. reviewed the manuscript; J.Y.W. conceived, designed and analyzed the study and wrote the manuscript.

**Non-author contributions and disclosures:** No;

**Agreement to Share Publication-Related Data and Data Sharing Statement:** Microarray data are available in the ArrayExpress database ([www.ebi.ac.uk/arrayexpress](http://www.ebi.ac.uk/arrayexpress)) under accession number E-MTAB-4773. The whole-genome sequencing data are available in the US National Library of Medicine (NLM) under accession number PRJNA994161. CITE-seq data (RNA and ADT) have been deposited in ArrayExpress database at EMBL-EBI ([www.ebi.ac.uk/arrayexpress](http://www.ebi.ac.uk/arrayexpress)) under the accession number E-MTAB-9803.

**Clinical trial registration information (if any):**

**Figure 1**

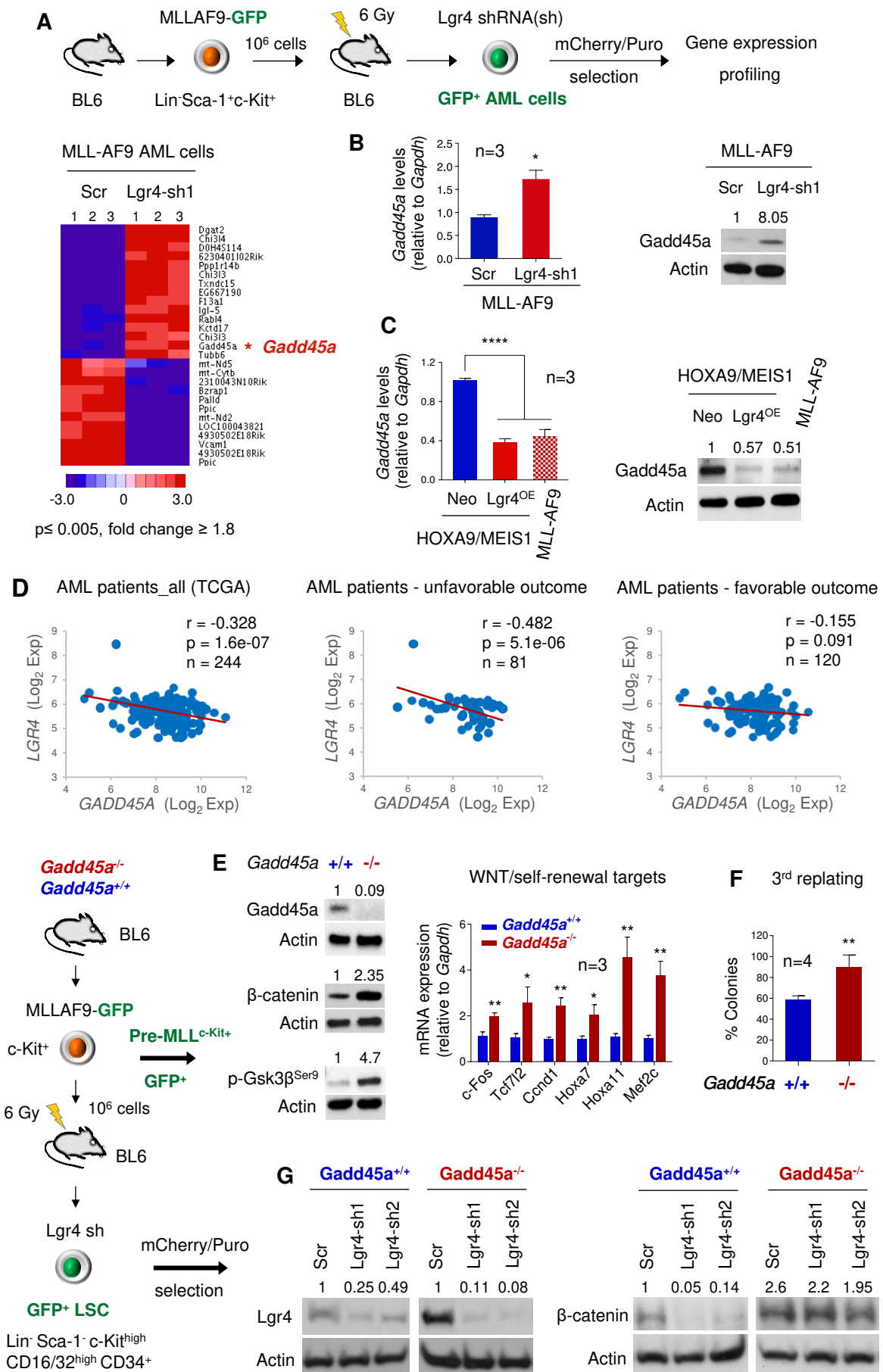


**Figure 2**

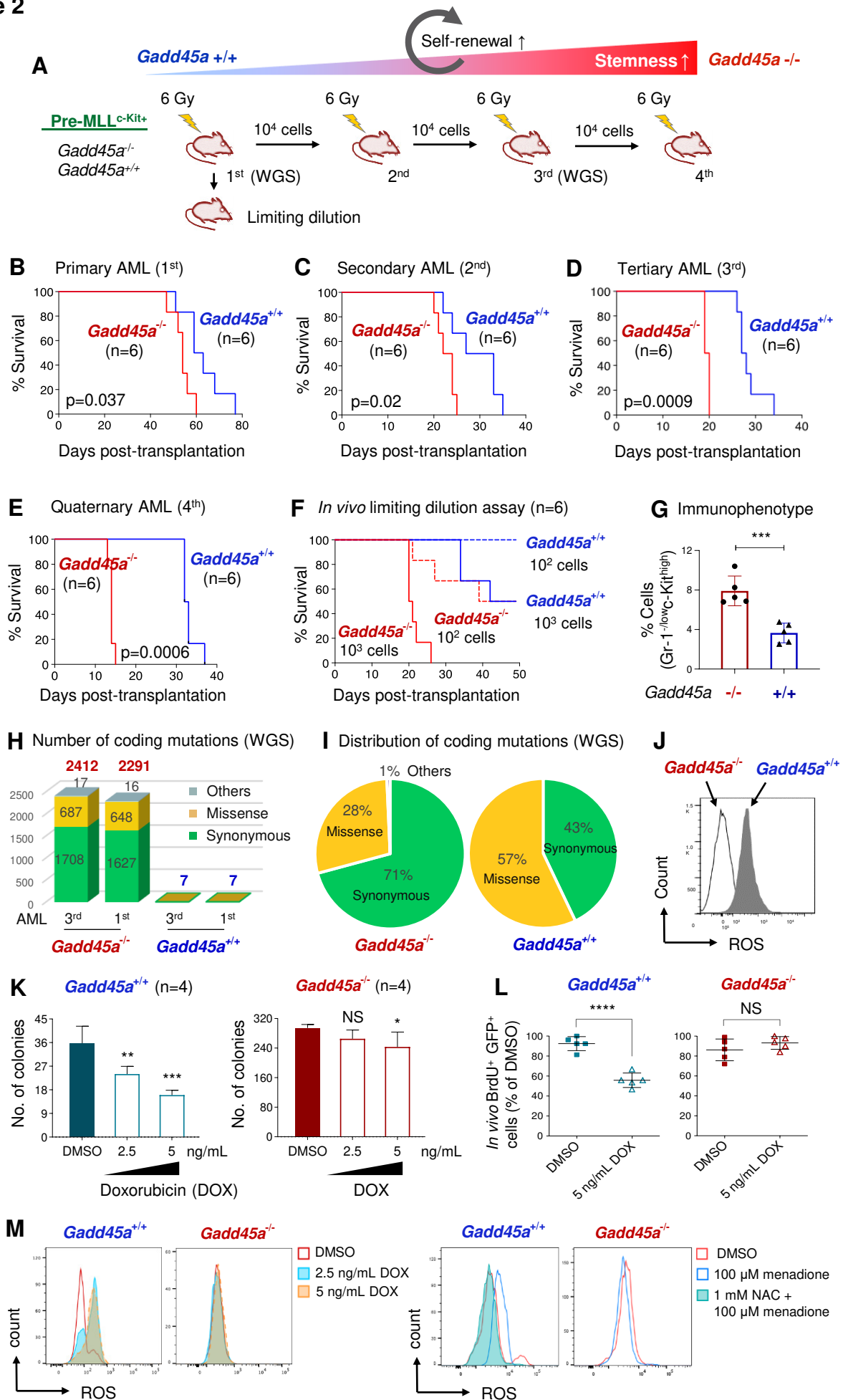


**Figure 3**

Establishment of *GADD45A* knockout (KO) PDX

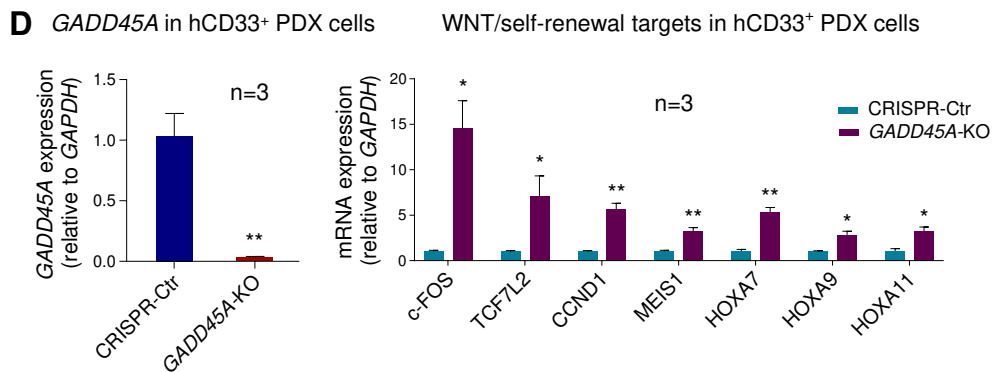
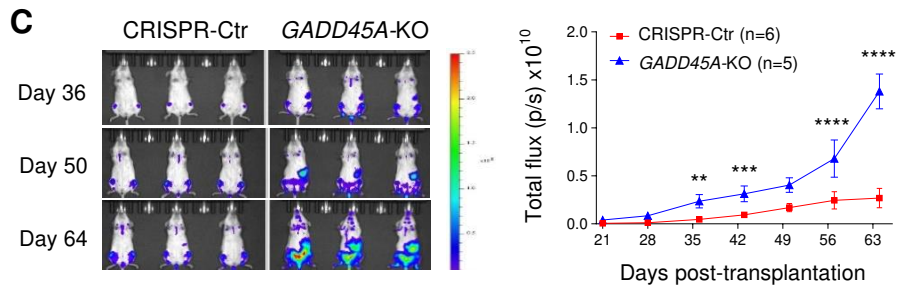
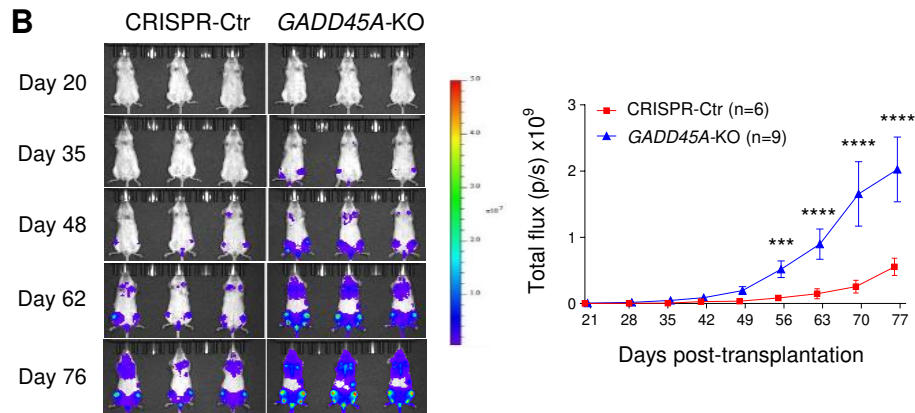
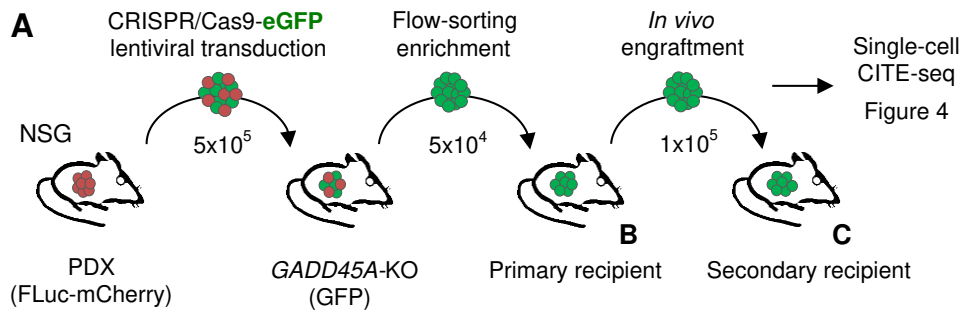


**Figure 4**

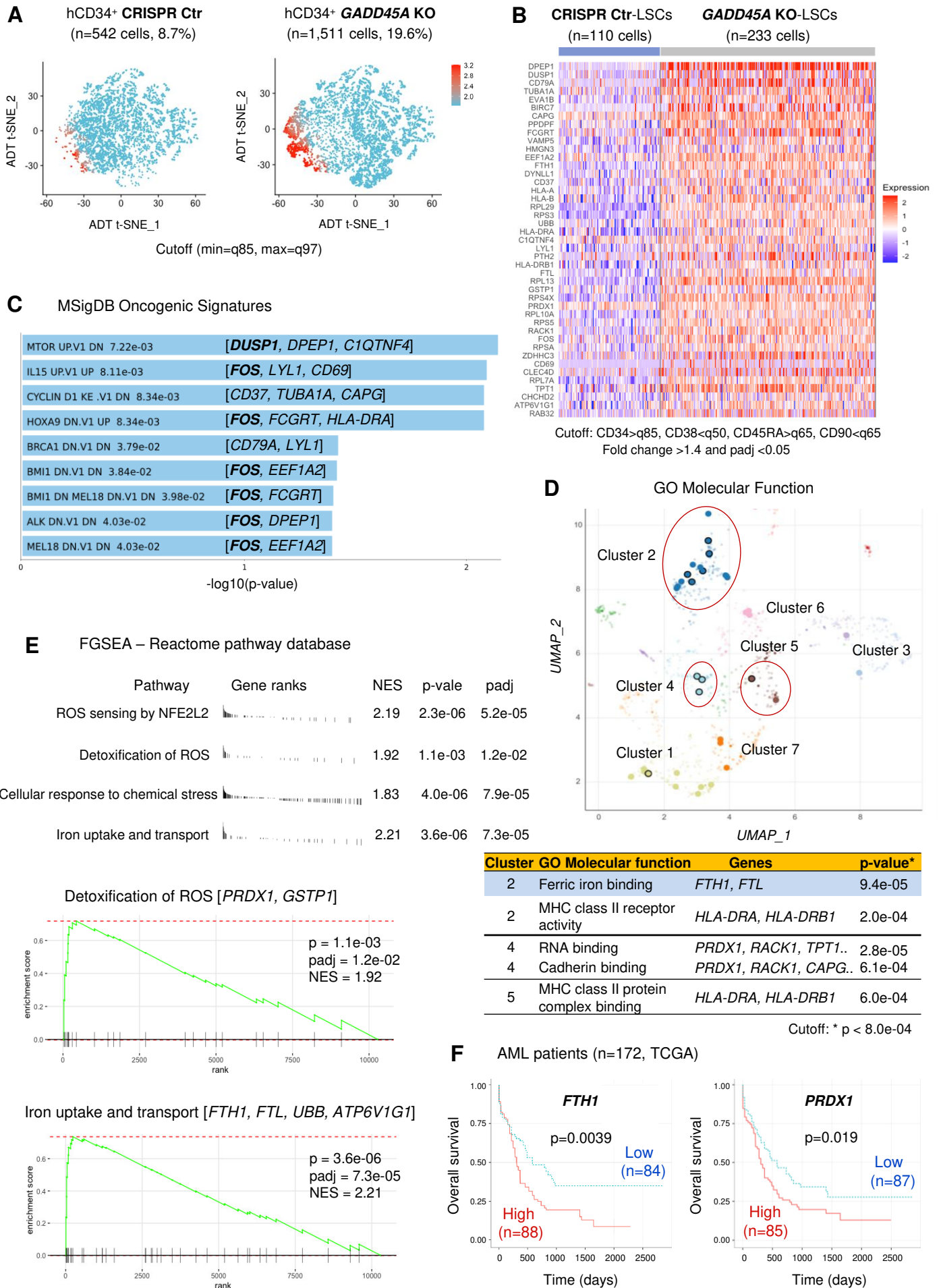


**Figure 5**

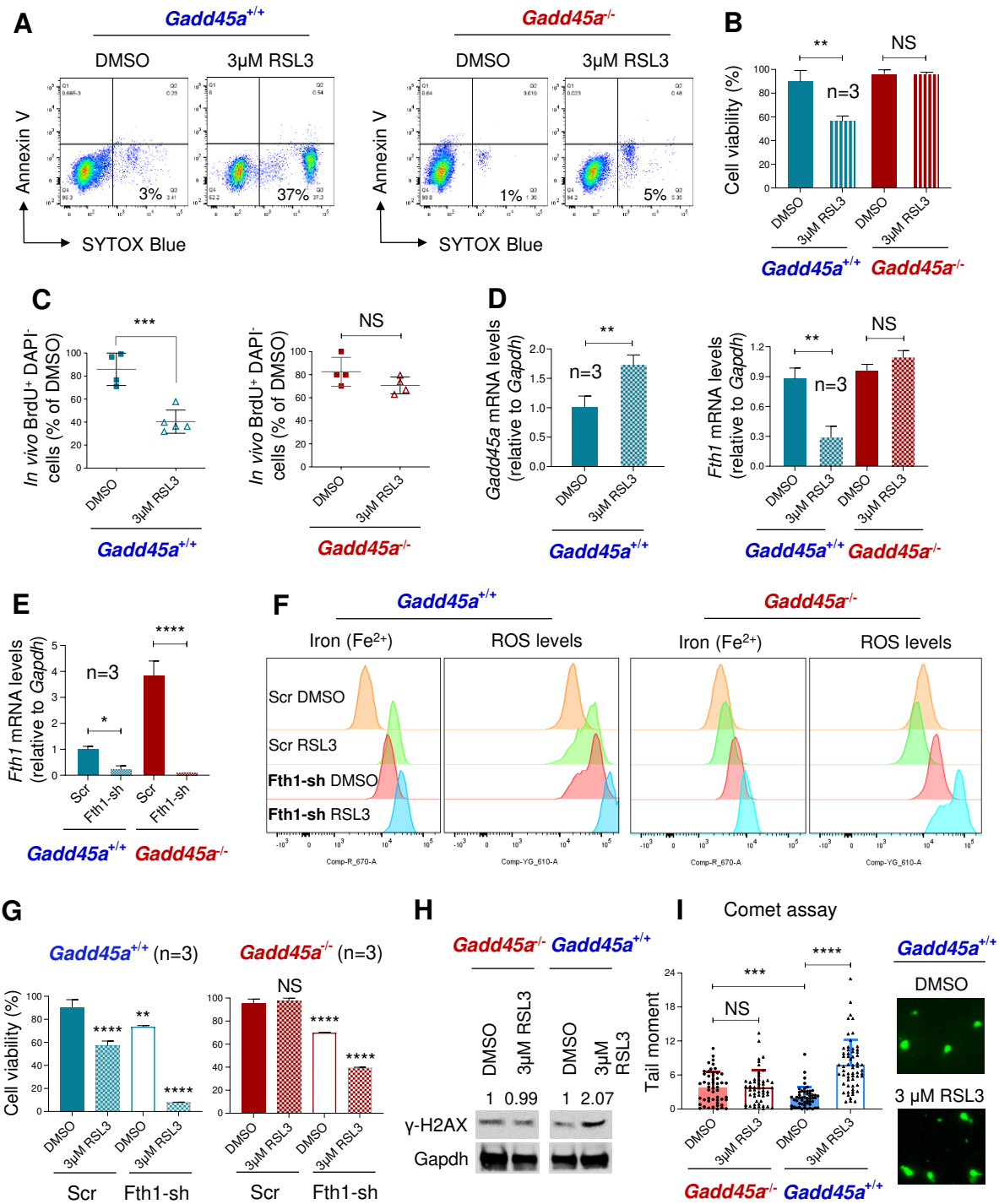
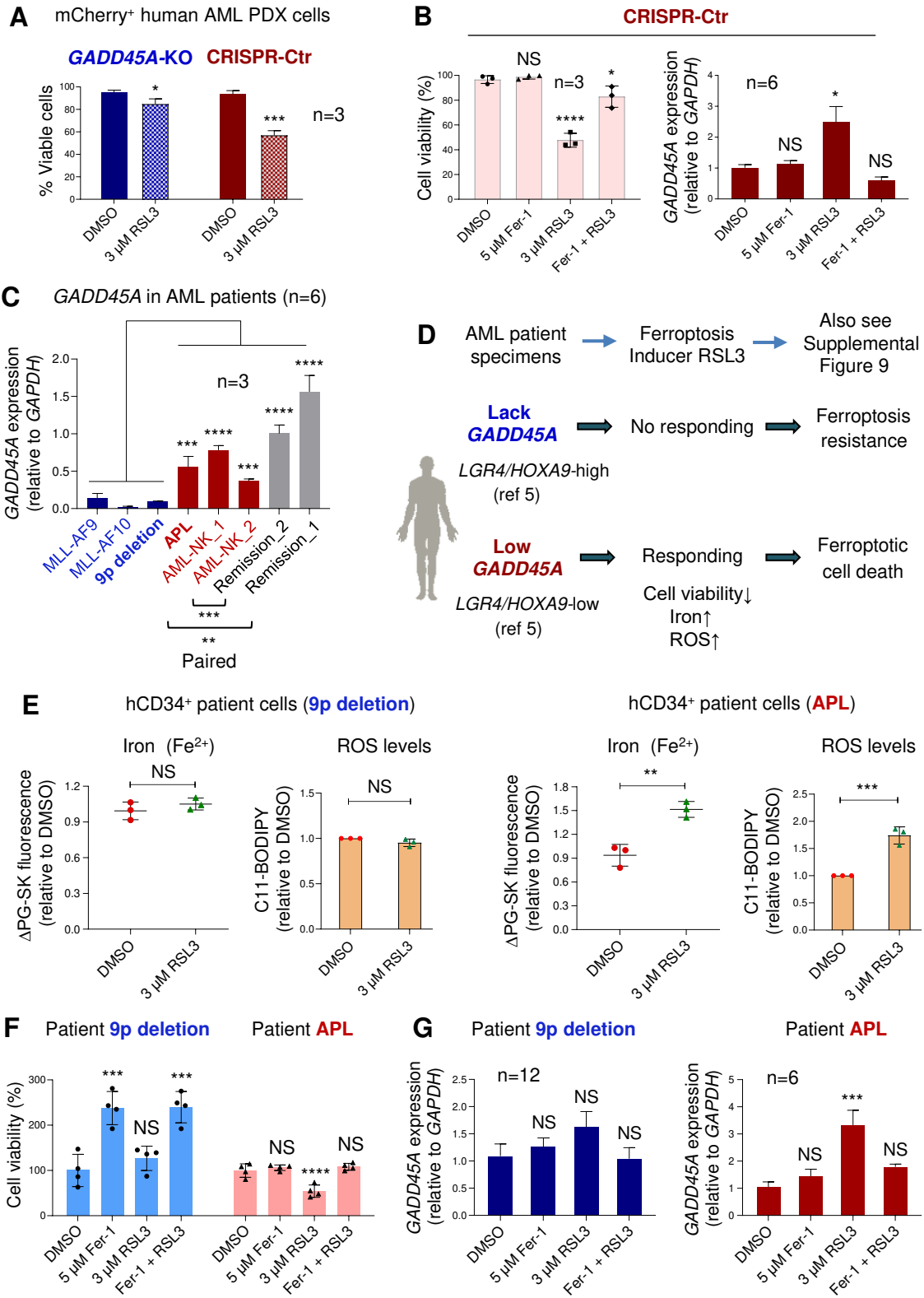


**Figure 6**





## MYELOID NEOPLASIA

### Loss of stress sensor GADD45A promotes stem cell activity and ferroptosis resistance in LGR4/HOXA9-dependent AML

**Short title:** GADD45A loss enhances stemness and resistance

Nunki Hassan,<sup>1#</sup> Hangyu Yi,<sup>1#</sup> Bilal Malik,<sup>1</sup> Lucie Gaspard-Boulinc,<sup>1,2</sup> Saumya E. Samaraweera,<sup>3</sup> Debora A. Casolari,<sup>3</sup> Janith Seneviratne,<sup>4</sup> Anushree Balachandran,<sup>4</sup> Tracy Chew,<sup>5</sup> Alastair Duly,<sup>4</sup> Daniel R. Carter,<sup>4</sup> Belamy B. Cheung,<sup>4</sup> Murray Norris,<sup>4</sup> Michelle Haber,<sup>4</sup> Maria Kavallaris,<sup>4,6</sup> Glenn M. Marshall,<sup>4,7</sup> Xu Dong Zhang,<sup>8,9</sup> Tao Liu,<sup>4</sup> Jianlong Wang,<sup>10</sup> Dan A. Liebermann,<sup>11</sup> Richard J. D'Andrea,<sup>3</sup> and Jenny Y. Wang<sup>1\*</sup>

#### Affiliations

<sup>1</sup>Cancer and Stem Cell Laboratory, School of Medical Sciences, Faculty of Medicine and Health, University of Sydney, Kolling Institute, Sydney, NSW 2006, Australia

<sup>2</sup>Department of Biology, Ecole normale supérieure, PSL University Paris, F-75005, Paris, France

<sup>3</sup>Acute Leukaemia Laboratory, Centre for Cancer Biology, University of South Australia and SA Pathology, Adelaide, South Australia, Australia

<sup>4</sup>Children's Cancer Institute, Lowy Cancer Research Centre, University of New South Wales, Sydney, NSW 2052, Australia

<sup>5</sup>Sydney Informatics Hub, Core Research Facilities, University of Sydney, NSW 2006, Australia

<sup>6</sup>Australian Centre for NanoMedicine and ARC Centre of Excellence in Convergent Bio-Nano-Science and Technology, University of New South Wales, Sydney, NSW 2052, Australia

<sup>7</sup>Kids Cancer Centre, Sydney Children's Hospital, Randwick 2031, New South Wales, Australia.

<sup>8</sup>School of Biomedical Sciences and Pharmacy, The University of Newcastle, NSW 2308, Australia

<sup>9</sup>Translational Research Institute, Henan Provincial People's Hospital and People's Hospital of Zhengzhou University, Academy of Medical Science, Zhengzhou University, Henan, 450053, China

<sup>10</sup>Department of Medicine, Columbia Center for Human Development, Columbia University Irving Medical Center, New York, NY 10032, USA

<sup>11</sup>Fels Institute for Cancer Research and Molecular biology and Department of Medical Genetics & Molecular Biochemistry, School of Medicine, Temple University, Philadelphia, PA19140, USA

# Equal contributions

\***Correspondence:** Jenny Y. Wang, e-mail: jenny.wang@sydney.edu.au

Microarray data are available in the ArrayExpress database ([www.ebi.ac.uk/arrayexpress](http://www.ebi.ac.uk/arrayexpress)) under accession number E-MTAB-4773. The whole-genome sequencing data are available in the US National Library of Medicine (NLM) under accession number PRJNA994161. CITE-seq data (RNA and ADT) have been deposited in ArrayExpress database at EMBL-EBI ([www.ebi.ac.uk/arrayexpress](http://www.ebi.ac.uk/arrayexpress)) under the accession number E-MTAB-9803.

## Key Points

- *GADD45A* loss has a dual role in promoting DNA damage while upregulating antioxidants to sustain low ROS essential to safeguard self-renewal
- Deletion of *GADD45A* enhances leukemia-initiating activity and therapy resistance by suppressing iron and ROS accumulation and ferroptosis

## Abstract

The overall prognosis of acute myeloid leukemia (AML) remains dismal, largely due to the inability of current therapies to kill leukemia stem cells (LSCs) with intrinsic resistance. Loss of the stress sensor *GADD45A* is implicated in poor clinical outcomes but its role in LSCs and AML pathogenesis is unknown. Here we define *GADD45A* as a key downstream target of LGR4 oncogenic signaling and discover a regulatory role for *GADD45A* loss in promoting leukemia-initiating activity and oxidative resistance in LGR4/HOXA9-dependent AML, a poor prognosis subset of leukemia. Knockout of *GADD45A* enhances AML progression in murine and patient-derived xenograft (PDX) mouse models. Deletion of *GADD45A* induces substantial mutations, increases LSC self-renewal and stemness *in vivo*, and reduces levels of reactive oxygen species (ROS), accompanied by a decreased response to ROS-associated genotoxic agents (e.g., ferroptosis inducer RSL3) and acquisition of an increasingly aggressive phenotype upon serial transplantation in mice. Our single-cell CITE-seq analysis on patient-derived LSCs in PDX mice and subsequent functional studies in murine LSCs and primary AML patient cells show that loss of *GADD45A* is associated with resistance to ferroptosis (an iron-dependent oxidative cell death caused by ROS accumulation) through aberrant activation of antioxidant pathways related to iron and ROS detoxification such as *FTH1* and *PRDX1*, upregulation of which correlates with unfavorable outcomes in AML patients. These results reveal a therapy resistance mechanism contributing to poor prognosis and support a role for *GADD45A* loss as a critical step for leukemia-initiating activity and as a target to overcome resistance in aggressive leukemia.

## Introduction

Acute myeloid leukemia (AML) is a heterogeneous and malignant clonal disease initiated by self-renewing leukemia stem cells (LSCs) arising from the transformation of hematopoietic stem cells (HSCs) or committed progenitor cells.<sup>1</sup> Pre-leukemic cells transformed from HSCs by oncogenes (e.g., MLL-AF9) can develop a highly aggressive subtype of AML with chemoresistance and expressing genes associated with inferior survival in AML patients.<sup>2,3</sup> Current chemotherapy is insufficient in targeting the intrinsic self-renewal mechanism in LSCs, which are a source of therapy resistance and relapse in AML.<sup>4</sup> We have previously shown that the heterogeneity of LSC self-renewal potential can be driven by distinct or partially overlapping regulatory mechanisms, where the interaction of G protein-coupled receptor LGR4 and its ligand R-Spondin 3 (RSPO3) is required for regulation of HSC-derived LSCs through  $\beta$ -catenin activation in AML that depends on HOXA9, a predictor of poor prognosis in a wide variety of human malignancies.<sup>5-10</sup> High LSC activity in a heterogeneous LSC pool is associated with poor clinical response to therapy.<sup>11,12</sup> It is thus of critical importance to identify key regulators that control leukemia-initiating cell activity essential for acquisition of an aggressive leukemia phenotype and therapeutic resistance.

Here we found that LGR4 negatively regulates GADD45A, which acts as a crucial stress sensor in response to replication stress-induced DNA damage and genotoxic stress-induced ferroptosis. Inhibition of Lgr4 in HSC-derived leukemic cells induces Gadd45a expression and deletion of *Gadd45a* in AML LSCs prevents the reduction of  $\beta$ -catenin induced by Lgr4 depletion, thus impacting a key regulator of self-renewal in hematopoietic development and malignancies. *Gadd45a*-deleted mice have a normal hematologic phenotype but display genomic instability, impairment in DNA repair, and accumulation of DNA damage and mutations in HSCs.<sup>13,14</sup> This is in line with our observation in LSCs, where deletion of *Gadd45a* causes mutations in DNA repair genes and replication stress while upregulating antioxidants to attenuate stress-induced ROS and iron production, leading to resistance to ferroptosis (an iron- and ROS-dependent cell death)<sup>15</sup>. DNA methylation of *GADD45A* is predictive of poor overall survival in AML and is associated with *DNMT3A* and *IDH1/2* mutations, while downregulation of *GADD45A* via *FLT3-ITD* mutation contributes to the myeloid differentiation block.<sup>16,17</sup> In contrast, elevated *GADD45A*

expression in normal HSCs induces differentiation via activation of p38 MAPK signaling that leads to the removal of damaged HSCs preventing malignant transformation.<sup>14,18</sup> GADD45A thus acts in a cell context-specific manner and is differentially required in normal and malignant hematopoiesis. However, the functional consequence of *GADD45A* loss in AML, especially in LSCs, has been largely unexplored.

## Materials and methods

Additional details are provided in the Supplemental Methods.

## Mice

Generation and use of *Gadd45a* knockout (*Gadd45a*<sup>-/-</sup>) and wild-type (*Gadd45a*<sup>+/+</sup>) mice have been described previously.<sup>19</sup> MLL-AF9 AML mouse models and patient-derived xenografts (PDX) were established by transplanting leukemic cells into female C57BL/6 (BL6) or NOD.Cg-Prkdc<sup>scid</sup> Il2rg<sup>tm1Wjl</sup>/SzJ (NSG) mice (Australian BioResources), as previously described.<sup>5,8,10,20</sup> All animal studies were in strict compliance with the Institutional Animal Care and Ethics Committee approved protocols. All animal studies were in strict compliance with the Institutional Animal Care and Ethics Committee approved protocols.

## Results

### **GADD45A is downregulated in Lgr4 pathway acting downstream of LGR4/p-PKAc/p-FOXO3A**

Using a stringent cutoff, our microarray data identified 15 genes upregulated by shRNA-mediated *Lgr4* knockdown (*Lgr4*-sh1)<sup>5</sup> in MLL-AF9-induced AML. Briefly, leukemic cells were generated by transducing HSC-enriched LSK cells (*Lin*<sup>-</sup>*Sca-1*<sup>+</sup>*c-Kit*<sup>+</sup>)<sup>1</sup> with MLL-AF9-GFP and transplanting resultant preleukemic cells into sublethally irradiated C57BL/6 (BL6) syngeneic mice. After developing AML, GFP<sup>+</sup> leukemic cells flow-sorted from mouse bone marrow (BM) were lentivirally transduced with *Lgr4* shRNA and selected for the microarray experiment (**Figure 1A; Supplemental Figure 1A**).

Among 15 upregulated genes, *Gadd45a* has been reported to negatively regulate  $\beta$ -catenin activity in epithelial tumors through promoting Gsk3 $\beta$  activation via dephosphorylation of Ser9.<sup>21</sup> We found that Lgr4 depletion increased *Gadd45a* expression in leukemic cells (**Figure 1B**). We have recently documented an indispensable role for Lgr4 in regulating self-renewal through cooperation with *Hoxa9* in aggressive AML.<sup>5</sup> Overexpression of Lgr4 (Lgr4<sup>OE</sup>) in HOXA9/MEIS1-transformed LSK cells not only produces leukemia with a shortened latency similar to that in MLL-AF9-induced AML, but also upregulates  $\beta$ -catenin reaching a level comparable to that in MLL-AF9-transformed LSK cells.<sup>5</sup> Consistently, overexpression of Lgr4 downregulated *Gadd45a* in HOXA9/MEIS1 leukemic cells, reaching a level similar to that in MLL-AF9 leukemic cells (**Figure 1C; Supplemental Figure 1B**). This is in line with a negative correlation between *LGR4* and *GADD45A* in 244 AML patients from The Cancer Genome Atlas (TCGA) dataset<sup>22</sup> that was mainly attributed to patients with unfavorable outcome (**Figure 1D**). These data indicate LGR4 as a negative regulator of GADD45A in poor-prognosis AML.

We next investigated the mechanism for Lgr4-mediated downregulation of *Gadd45a*. The TCGA dataset revealed a positive correlation between *FOXO3* and *GADD45A* (**Supplemental Figure 1C**), which was consistent with a negative correlation between *LGR4* and *GADD45A* in AML patients with unfavorable outcome (**Figure 1D**). This implicates FOXO3-mediated regulation of GADD45A in poor-prognosis AML. Knockdown of Lgr4 decreased the phosphorylation of FoxO3a in MLL-AF9 LSCs (Lin<sup>-</sup>Sca-1<sup>c-</sup>Kit<sup>high</sup>CD16/32<sup>high</sup>CD34<sup>+</sup>)<sup>1</sup> (**Supplemental Figure 1D**). The phosphorylation of FOXO3A, and its consequent cytoplasmic localization and inactivation, is a poor prognostic factor in AML, particularly those with FLT3 mutations.<sup>23</sup> Consistent with the role of p-PKAc as a downstream effector of Lgr4 pathway,<sup>5</sup> the specific inhibitor of PKA, PKI, reduced the phosphorylation of FoxO3a leading to increased *Gadd45a* in MLL-AF9 LSCs and in human MLL-AF9 AML (THP-1) cells (**Supplemental Figure 1E-F**). These results support p-PKAc/p-FOXO3A-mediated downregulation of GADD45A.

### ***GADD45A* loss increases the WNT/self-renewal activity through phosphorylation of GSK3 $\beta$**

To define a direct role for *Gadd45a* loss in Lgr4/ $\beta$ -catenin signaling, we tested the effect of *Gadd45a* deletion on Wnt/ $\beta$ -catenin activity in MLL-AF9-GFP transformed HSC/progenitor-enriched c-Kit<sup>+</sup> cells<sup>10</sup>, which were isolated from the BM of *Gadd45a* knockout mice<sup>19</sup>. Compared to wild-type *Gadd45a* (*Gadd45a*<sup>+/+</sup>), deletion of *Gadd45a* (*Gadd45a*<sup>-/-</sup>) in GFP<sup>+</sup> pre-leukemic MLL-AF9 cells (pre-MLL<sup>c-Kit+</sup>) increased endogenous  $\beta$ -catenin and inactivated/phosphorylated Gsk3 $\beta$  (p-Gsk3 $\beta$ <sup>Ser9</sup>), while upregulating key self-renewal signature genes such as WNT/ $\beta$ -catenin targets (*c-Fos*, *Tcf7l2* and *Ccnd1*)<sup>5</sup> and MLL-fusion targets (*Mef2c* and HoxA cluster genes *Hoxa7* and *Hoxa11*)<sup>1</sup> (**Figure 1E**). In contrast, knockdown of  $\beta$ -catenin repressed expression of self-renewal signature genes and reduced colony formation in *Gadd45a*<sup>-/-</sup> cells (**Supplemental Figure 1G**). *Gadd45a*<sup>-/-</sup> cells exhibited enhanced serial-replating capacity, indicative of increased self-renewal (**Figure 1F**), whereas overexpression of *Gadd45a* inhibited leukemic cell growth (**Supplemental Figure 1H**). Likewise, knockdown of LGR4 in human AML (THP-1) cells elevated endogenous GADD45A expression, while deletion of *GADD45A* via CRISPR/Cas9 increased inactive p-GSK3 $\beta$ <sup>Ser9</sup> and nuclear non-phospho (active)  $\beta$ -catenin as well as key WNT/self-renewal target genes (**Supplemental Figure 2A-D**). To further determine the role of *Gadd45a* loss as a downstream effector of LGR4 signaling, we generated *Gadd45a*<sup>+/+</sup> versus *Gadd45a*<sup>-/-</sup> LSCs expressing or depleting Lgr4, by transplanting pre-MLL<sup>c-Kit+</sup> cells into syngeneic mice to develop AML followed by lentiviral transduction of LSCs with Lgr4 shRNAs. We observed that knockdown of Lgr4 with two independent shRNAs (sh1 and sh2)<sup>5</sup> decreased  $\beta$ -catenin expression in *Gadd45a*<sup>+/+</sup> LSCs, but not in *Gadd45a*<sup>-/-</sup> LSCs (**Figure 1G**). These data suggest that loss of *GADD45A* sustains  $\beta$ -catenin levels and WNT/self-renewal activity through phosphorylation of GSK3 $\beta$ , acting downstream of LGR4 signaling.

### **Deletion of *GADD45A* enhances self-renewal and leukemic potential upon serial transplantation**

We assessed the impact of *Gadd45a* loss on AML pathogenesis *in vivo*, and observed a significantly shortened latency for the mice transplanted with *Gadd45a*<sup>-/-</sup> compared to *Gadd45a*<sup>+/+</sup> pre-MLL<sup>c-Kit+</sup> cells (primary AML, **Figure 2A-B**; **Supplemental Figure 3A**). This suggests that *Gadd45a* loss promotes leukemia progression. To test the role of *Gadd45a* loss in regulating the self-renewal and frequency of

LSCs *in vivo*, we performed serial transplantation and limiting-dilution assays. GFP<sup>+</sup> MLL-AF9 leukemic cells flow-sorted from mice with primary AML were serially transplanted into syngeneic recipient mice. *Gadd45a*<sup>-/-</sup> leukemic cells gradually shortened disease latencies upon serial transplantation in mice (secondary/tertiary/quaternary AML, **Figure 2C-E**) compared with *Gadd45a*<sup>+/+</sup> cells, consistent with a progressively increasing self-renewal potential and an aggressive phenotype similar to that of relapsed human MLL-rearranged AML. *In vivo* limiting-dilution assay showed that deletion of *Gadd45a* caused a 10-fold increase in LSC frequency in *Gadd45a*<sup>-/-</sup> compared to *Gadd45a*<sup>+/+</sup> mice (1/142 and 1/1650,  $p=0.00114$ ; **Figure 2F**). Likewise, immunophenotypic analysis revealed a 2-fold increase of Gr-1<sup>-low</sup>c-Kit<sup>high</sup> LSC-enriched population in *Gadd45a*<sup>-/-</sup> compared to *Gadd45a*<sup>+/+</sup> leukemic cells (**Figure 2G**; **Supplemental Figure 3B**). We have previously documented that the Gr-1<sup>-low</sup>c-Kit<sup>high</sup> population is over 100-fold enriched for LSCs compared with the Gr-1<sup>+</sup>c-Kit<sup>high</sup> population in a heterogeneous LSC pool of AML.<sup>10</sup> Loss of *GADD45A* thus results in leukemia-initiating cell enrichment and increased LSC frequency, consistent with a correlation between high LSC frequency at diagnosis and poor prognosis in AML patients.<sup>11</sup>

### ***GADD45A* loss induces replication stress and mutations in DNA repair and self-renewal genes**

As *Gadd45a*<sup>-/-</sup> mice exhibit decreased DNA repair and increased mutation frequency,<sup>13</sup> we examined whether deletion of *Gadd45a* promoted AML progression by inducing genomic instability and mutations. Our whole-genome sequencing (WGS) of LSCs from primary and tertiary AML showed that deletion of *Gadd45a* induced substantial mutations (**Figure 2H-I**), particularly missense mutations involved in DNA repair (*Ddx11*, *Rad21*),<sup>24</sup> self-renewal (HoxA clusters: *Hoxa4*, *Hoxa5*, *Hoxa9*, *Hoxa10*),<sup>1</sup> and DNA methylation (*Dnmt1*)<sup>25</sup> (**Supplemental Figure 3C**). Sanger sequencing confirmed persistent missense variants of *Hoxa5* and *Hoxa9* induced by *Gadd45a* deletion in LSCs from primary and tertiary AML (**Supplemental Figure 3D**), demonstrating the accuracy of WGS data. Notably, *Gadd45a* deletion induced not only a missense mutation in exon 21 of the *Ddx11* gene but also multiple synonymous mutations in exons 19-26, leading to decreased expression of *Ddx11* (**Supplemental Figure 3E**). Since *Ddx11* is a DNA helicase essential for double-strand break repair during DNA

replication,<sup>24</sup> loss of *Gadd45a* likely causes replication stress through DNA repair gene variants, leading to genomic instability and DNA damage accumulation in LSCs. Since no additional mutations were found in key *Gadd45a* targets over serial transplantation, the enhancement of the leukemic potential in *Gadd45a*<sup>-/-</sup> mice was likely due to increased self-renewal, associated with HoxA cluster gene variants, that endowed LSCs with a competitive advantage. This finding aligns with our recent discovery demonstrating a positive cooperation between HOX and LGR4 pathways in promoting self-renewal and leukemic potential in LGR4/HOXA9-dependent AML.<sup>5</sup>

### ***GADD45A* loss fosters stem cell features driving resistance to therapy-associated oxidative stress**

We next examined the role of *Gadd45a* loss as a determinant of therapy resistance in LSCs. Compared to *Gadd45a*<sup>+/+</sup> LSCs, *Gadd45a*<sup>-/-</sup> LSCs exhibited a lower level of ROS and a higher proportion of quiescent G0 cells (**Figure 2J**; **Supplemental Figure 3F**), which are critical features associated with increased resistance to therapy.<sup>26</sup> Consistently, treatment with the chemotherapeutic agent doxorubicin (a mainstay of AML therapy producing high levels of ROS) had little effects on *Gadd45a*<sup>-/-</sup> LSCs but reduced the colony-forming capacity of *Gadd45a*<sup>+/+</sup> LSCs (**Figure 2K**). Subsequent cell proliferation assay at 12 days post-injection of mice, following *ex vivo* pre-treatment with doxorubicin, revealed impaired proliferation of *Gadd45a*<sup>+/+</sup> LSCs, but not *Gadd45a*<sup>-/-</sup> LSCs (**Figure 2L**). This is consistent with aberrant ROS production induced by doxorubicin or menadione (ROS inducer) but rescued by N-acetylcysteine (ROS scavenger) in *Gadd45a*<sup>+/+</sup> LSCs, rather than *Gadd45a*<sup>-/-</sup> LSCs (**Figure 2M**), underlining ROS-specific and *Gadd45a*-dependent effects. These data support a protective role of *GADD45A* loss against chemotherapy-associated oxidative stress in LSCs, and underscore the importance of *GADD45A* expression in determining LSC properties essential for leukemia progression and therapy resistance.

### **Deletion of *GADD45A* increases tumor burden in AML patient-derived xenograft mice**

We have recently demonstrated that RSPO3-LGR4 activation is required for LSC survival in patient-derived xenograft (PDX) mouse model of relapsed AML harboring mutations including *DNMT3A*,



*RUNX1* and *K/NRAS*.<sup>5</sup> Here we investigated the impact of *GADD45A* loss on AML progression in established PDXs expressing firefly luciferase (FLuc) and mCherry. We found that deletion of *GADD45A* by CRISPR/Cas9 caused increased AML burden, as determined by FLuc-based bioluminescence imaging in PDX mice (**Figure 3A-B; Supplemental Figure 4A-B**). Subsequent secondary transplantation in NSG mice showed that *GADD45A* deletion enhanced the long-term leukemia-initiating activity of AML cells, which was associated with increased WNT/self-renewal signature (**Figure 3C-D**). This supports the role for *GADD45A* loss in promoting *in vivo* engraftment of human AML cells and leukemia-initiating activity.

### ***GADD45A* loss upregulates pathways involved in self-renewal and antioxidant defense at single-cell level**

To understand how loss of *GADD45A* contributes to therapy resistance in aggressive AML, we performed CITE-seq (cellular indexing of transcriptomes and epitopes by sequencing)<sup>27</sup> that used DNA-barcoded antibodies to tag cell-surface markers of human LSCs, enabling simultaneous quantification of mRNA and ADT (antibody-derived tag) on a given single cell. Our results showed that the LSC compartment (CD34<sup>+</sup>CD38<sup>-</sup>CD90<sup>+</sup>CD45RA<sup>+</sup>)<sup>28</sup> in human AML PDX cells was enriched specifically in cluster 2 (**Supplemental Figure 5A-B**). Deletion of *GADD45A* resulted in a 3-fold increase in the LSC-enriched CD34<sup>+</sup> population and a 2-fold increase in the LSC compartment (**Figure 4A-B**). Single-cell transcriptomic profiling identified 43 differentially expressed genes (DEGs) upregulated in *GADD45A*-deleted LSCs compared with CRISPR-control LSCs, including genes associated with LSC survival and self-renewal (e.g., *DUSP1* and *c-FOS*),<sup>29,30</sup> iron detoxification and storage (e.g., ferritin heavy/light chain FTH1/FTL)<sup>31,32</sup> (**Figure 4B; Supplemental Figure 5C**). Pathway enrichment analysis of DEGs using MSigDB uncovered several self-renewal pathways including the HOXA9 pathway (e.g., *c-FOS*) (**Figure 4C**). Strikingly, *c-FOS*, as a key WNT/ $\beta$ -catenin target that directly interacts with  $\beta$ -catenin for transcriptional activation of downstream components,<sup>33</sup> was present in most of the top 9 oncogenic pathways implicating its crucial role in *GADD45A* loss-mediated  $\beta$ -catenin self-renewal activation. Subsequent Gene Ontology (GO) analysis showed that the DEGs were enriched in molecular function

(**Figure 4D**), particularly in iron ion binding (e.g., *FTH1* and *FTL*). Likewise, our fast pre-ranked gene set enrichment analysis (FGSEA) of the Reactome pathway database identified *GADD45A* loss-induced enrichment of antioxidant-related gene sets including iron uptake and transport (e.g., *FTH1* and *FTL*) and ROS sensing/detoxification (e.g., *PRDX1*, *GSTP1*)<sup>34,35</sup> (**Figure 4E**). These observations agree with reduced ROS levels and increased self-renewal in *GADD45A*-deleted LSCs, underlining a possible involvement of *GADD45A* loss in antioxidant defense against iron and ROS accumulation (a defining feature of ferroptosis).<sup>15</sup>

Our analysis of TCGA AML dataset<sup>22</sup> revealed a correlation between high expression of antioxidants *FTH1* and *PRDX1* with unfavorable outcomes in a cohort of 172 AML patients (**Figure 4F**). This is in line with a recent report showing that high levels of *FTH1* and *FTL* in a cohort of 525 AML patients are associated with chemoresistance and enrichment of genes related to oxidative stress and iron pathways.<sup>36</sup> Likewise, our functional studies showed that knockdown of *GADD45A* induced endogenous *FTH1* expression (**Supplemental Figure 6A**). Overexpression of *FTH1* reduced intracellular ROS and iron, whereas knockdown of *FTH1* elevated ROS levels in human AML (THP-1) cells (**Supplemental Figure 6B-D**). These data suggest *FTH1* acting downstream of *GADD45A* loss to provide antioxidant defense against iron and ROS accumulation.

### ***GADD45A* loss protects against ferroptosis by upregulating *FTH1*-mediated antioxidant defense**

We next explored the role for *GADD45A* loss in preventing ferroptosis through upregulation of *FTH1*. RSL3 (a selective ferroptosis inducer)<sup>37</sup> triggered ferroptotic/non-apoptotic cell death and reduced *in vitro* colony-forming capacity and *in vivo* cell proliferation in *Gadd45a*<sup>+/+</sup> LSCs, rather than *Gadd45a*<sup>-/-</sup> LSCs, from mice with tertiary AML (**Figure 2D, 5A-C**). The sensitivity of *Gadd45a*<sup>+/+</sup> LSCs to RSL3 treatment could be attributed to the ability of RSL3 to induce *Gadd45a* expression and reduce *Fth1* in *Gadd45a*<sup>+/+</sup> LSCs, but not *Gadd45a*<sup>-/-</sup> LSCs (**Figure 5D**). In support of this notion, knockdown of *Fth1* promoted RSL3-induced ferroptosis in both *Gadd45a*<sup>-/-</sup> and *Gadd45a*<sup>+/+</sup> LSCs revealing increased ROS and ferrous iron (Fe<sup>2+</sup>) accompanied by decreased cell viability (**Figure 5E-G**). This is in line with the

role of Fth1 acting downstream of *Gadd45a* loss to counteract RSL3-induced ROS and iron and consequently prevent genotoxic stress-induced DNA damage and ferroptosis. The protective effect of *Gadd45a* deletion against RSL3-induced exogenous DNA damage was demonstrated by the result of RSL3-induced increase in  $\gamma$ -H2AX (a biomarker for DNA double-strand breaks)<sup>38</sup> in *Gadd45a*<sup>+/+</sup> LSCs, but not in *Gadd45a*<sup>-/-</sup> LSCs, and by a similar result obtained from the alkaline comet assay (genotoxicity testing for DNA-strand breaks)<sup>39</sup> (**Figure 5H-I**). Notably, a higher level of endogenous DNA damage was observed in *Gadd45a*<sup>-/-</sup> than *Gadd45a*<sup>+/+</sup> LSCs (**Figure 5I**), consistent with the role of *Gadd45a* deletion in increasing replication stress and stress-induced DNA damage (**Figure 2H**). These data demonstrate *GADD45A* loss as a key determinant in preventing stress-induced DNA damage and RSL3-induced ferroptosis, primarily by upregulating FTH1-mediated antioxidant defense that scavenges excessively produced ROS and iron.

### **Suppression of *GADD45A* affects ferroptosis sensitivity in primary human AML cells**

To investigate the role of *GADD45A* loss in regulating ferroptosis resistance in human AML cells, we treated mCherry<sup>+</sup> PDX cells with RSL3. CRISPR/Cas9-mediated deletion of *GADD45A* prevented RSL3-induced ferroptosis; conversely, CRISPR-control PDX cells that expressed low levels of *GADD45A* responded to RSL3 treatment causing ~40% cell death (**Figure 6A; Supplemental Figure 7**). RSL3-induced ferroptosis could be rescued by pre-treatment with a ferroptosis inhibitor, ferrostatin-1 (Fer-1) that inhibits ferroptosis by reducing iron levels,<sup>15</sup> which suppressed RSL3-induced expression of endogenous *GADD45A* (**Figure 6B**). These results support *GADD45A* as a positive regulator of ferroptosis and deletion of *GADD45A* promotes ferroptosis resistance in human AML cells.

We further assessed the association of *GADD45A* expression with ferroptosis in primary AML patient specimens that express high levels of *LGR4/HOXA9* (9p deletion, MLL-AF10, MLL-AF9) versus relatively low levels of *LGR4/HOXA9* (acute promyelocytic leukemia or APL, AML with normal karyotype or AML-NK), as shown in our recent studies.<sup>5</sup> Lower expression of *GADD45A* was shown in *LGR4/HOXA9*-high than *LGR4/HOXA9*-low cells (**Figure 6C; Supplemental Figure 8A-B**). Lack of

endogenous *GADD45A* in AML with 9p deletion or MLL-AF10 rendered LGR4/HOXA9-high cells resistant to RSL3 treatment; conversely, expression of *GADD45A* in APL or AML-NK, even at much lower levels than paired remission samples, sensitized LGR4/HOXA9-low cells to RSL3 treatment leading to ferroptosis with increased iron and ROS accompanied by reduced cell viability (**Figure 6C-F; Supplemental Figure 9A-B**). RSL3 induced ferroptosis by upregulating *GADD45A* that could be suppressed by ferroptosis inhibitor Fer-1 in LGR4/HOXA9-low cells; however, RSL3 had no impact on LGR4/HOXA9-high cells that intrinsically lacked *GADD45A* (**Figure 6C-G**). This suggests a threshold level of endogenous *GADD45A* required for ferroptosis induction. These data underline a proactive role of *GADD45A* in RSL3-induced ferroptosis; loss of *GADD45A* provides a shield against this mechanism of cell death in aggressive AML that is dependent on *LGR4/HOXA9* expression.

## Discussion

LSCs exhibit functional heterogeneity, particularly in HSC-derived AML with adverse/intermediate-risk cytogenetics, characterized by high self-renewal and frequency of leukemia-initiating cells alongside low response to chemotherapy.<sup>2,3,5,40</sup> High LSC activity is associated with elevated relapse risk and poor survival in AML patients.<sup>11,12</sup> We have recently demonstrated an indispensable role for RSPO3-LGR4 signaling in the formation and function of HSC-derived LSCs through aberrant activation of p-PKAc/p-CREB/CBP-p300/ $\beta$ -catenin pathway, contributing to aggressive phenotypes in HOXA9-dependent AML.<sup>5</sup> Here, we identify *GADD45A* as a key negative regulator of leukemia-initiating activity and therapy resistance, acting downstream of LGR4/p-PKAc/p-FOXO3A. Loss of *GADD45A* in a heterogeneous LSC pool increases LSC self-renewal and frequency and decreases chemosensitivity, leading to a more aggressive AML phenotype. Several mechanisms may act in concert to promote *GADD45A* loss-associated leukemogenic potential: deletion of *GADD45A* increases WNT/ $\beta$ -catenin self-renewal activity (e.g., *c-FOS* and *HOXA* cluster) through GSK3 $\beta$  phosphorylation (inactivation), and induces replication stress and mutations in DNA repair and self-renewal genes contributing to enhanced cooperation of LGR4 and HOX pathways in promoting stemness and self-renewal, while conferring resistance to oxidative stress and ferroptosis via upregulation of FTH1-mediated antioxidant defense

that stores iron in a non-toxic form and scavenges excessive ROS production induced by replication stress or therapy-induced genotoxic stress.

ROS is an important determinant of stem cell fate. Low ROS closely correlates with increased self-renewal and quiescence in normal and malignant stem cells,<sup>26,41</sup> and a slight increase of intracellular ROS induces LSC differentiation.<sup>42</sup> Consistently, deletion of *GADD45A* in LSCs reduces ROS levels and promotes self-renewal in a mouse model of AML development; however, it also causes replication stress and DNA damage accumulation, which have the potential to increase ROS production.<sup>43</sup> This raises a critical question of how low ROS is sustained in LSCs under persistent DNA damage. Our single-cell CITE-seq data on patient-derived LSCs and subsequent functional studies directly link *GADD45A* deletion to aberrant activation of antioxidant defense against ROS and iron accumulation. *GADD45A* loss serves as a safeguard by upregulating FTH1-mediated antioxidant defense, which attenuates ROS generated by replication stress-induced DNA damage and thereby maintains ROS at a basal non-toxic low level to protect LSC compartment from oxidative stress.

Antioxidant defense upregulated by *GADD45A* loss also acts as the protective mechanism against genotoxic stress-induced iron and ROS accumulation in response to chemotherapeutic agent doxorubicin and ferroptosis inducer RSL3 leading to therapy resistance. Ferroptosis is an iron ( $\text{Fe}^{2+}$ )-dependent oxidative cell death caused by ROS generated through Fenton reaction and subsequent lipid peroxidation.<sup>15</sup> Ferroptosis resistance remains a significant challenge to therapeutic exploitation of the iron-dependent cell death mechanism. In this study, we identify *GADD45A* loss as a key regulator of ferroptosis resistance. Deletion of *GADD45A* in murine LSCs or lack of *GADD45A* in LGR4/HOXA9-dependent patient cells (indicative of poor outcome) renders cells resistant to ferroptosis induced by RSL3. Our pathway enrichment analysis uncovers abnormal activation of iron detoxification driven by ferritin (FTH1/FTL), an iron storage protein complex.<sup>31,32</sup> FTH1 has ferroxidase activity to convert  $\text{Fe}^{2+}$  to  $\text{Fe}^{3+}$  for iron storage in a non-toxic form via FTL that prevents excess  $\text{Fe}^{2+}$  to produce ROS via the Fenton reaction or by forming the doxorubicin- $\text{Fe}^{2+}$  complex.<sup>32,44</sup> Upregulation of *FTH1* is correlated with

unfavorable outcomes in AML patients, while FTH1 modulates intracellular iron and ROS levels acting downstream of GADD45A in AML LSCs. These findings underline a crucial role of *GADD45A* loss in therapy resistance by upregulating FTH1-mediated antioxidant defense that limits iron-dependent ROS production, allowing LSCs to survive under persistent genotoxic stress without surpassing a deadly threshold in a subgroup of leukemia with poor prognosis.

In addition to ferritin (FTH1/FTL) as an antioxidant defense system, our single-cell studies also uncover aberrant activation of pathways related to LSC survival (e.g., *DUSP1*) and antioxidants (e.g., *PRDX1* and *GSTP1*) in *GADD45A*-deleted human LSCs. Like *FTH1*, high expression of *PRDX1*, which can scavenge excess ROS and decreases damage from oxidative stress,<sup>34</sup> correlates with unfavorable prognosis in AML patients. The positive correlation between *FTH1* and *DUSP1* expression in AML patients from TCGA (**Supplemental Figure 10**) implies a possible cooperation between FTH1 and DUSP1 pathways in ferroptosis resistance and LSC survival, acting downstream of GADD45A. Thus, loss of *GADD45A* may play a crucial role in protecting leukemia-initiating cells against oxidative stress and ferroptosis by simultaneous modulation of multiple pathways, suggesting that targeting of individual downstream effectors may not be sufficient to fully restore GADD45A tumor-suppressor function. In this regard, therapeutic approaches to induce GADD45A expression in LSCs likely represent a more robust strategy to compromise LSC function and modulate cell sensitivity to anti-cancer agents associated with oxidative stress and ferroptosis.

Ferroptosis inducers may be one approach to promote GADD45A expression in AML cells expressing this gene even at very low levels, but are unable to restore GADD45A in cells lacking its expression. This is because a threshold level of endogenous GADD45A is required for ferroptosis induction. Alternative approaches are needed for AML cells lacking GADD45A. Given our findings that LGR4 pathway inhibition induces GADD45A expression and GADD45A acts downstream of LGR4/p-PKAc/p-FOXO3, restoring GADD45A in LSCs can be achieved by blocking this pathway in a significant group of AML. In particular, we observe the lack of *GADD45A* in primary patient specimens expressing high *LGR4/HOXA9*, which critically depend on RSPO3-LGR4 activation for LSC survival and maintenance of

myeloid undifferentiated state.<sup>5</sup> We have recently demonstrated that a clinical-grade anti-RSPO3 antibody specifically targets LGR4 signaling via disruption of the RSPO3-LGR4 interaction, which compromises *in vivo* leukemia-initiating activity in primary AML PDX mouse models that harbor high-risk cytogenetics (e.g., MLL-AF9 or 9p deletion)<sup>5</sup> and lack *GADD45A*. Notably, we found that *in vivo* anti-RSPO3 antibody treatment induced endogenous *GADD45A* in NSG mice engrafted with primary MLL-AF9 AML patient cells (**Supplemental Figure 11A-C**), thereby offering a potential strategy to overcome resistance to ferroptosis. Nevertheless, we cannot exclude the possibility of other factors such as DNA methylation in coordinately regulating *GADD45A*. We have previously shown that LGR4 decreased intracellular ROS,<sup>5</sup> which affects DNA methylation by acting on the activity/expression of DNA methyltransferases (DNMTs).<sup>45</sup> The DNMT inhibitor, decitabine that predominantly inhibits DNMT1 activity,<sup>46</sup> induced *GADD45A* expression in MLL-AF9 LSCs (**Supplemental Figure 11D**). This indicates a coordinated downregulation of *GADD45A* in LGR4/HOXA9-dependent LSCs by multiple mechanisms including LGR4/p-PKAc/p-FoxO3a and DNA methylation.

In summary, we have identified a key regulatory role for *GADD45A* loss in promoting LSC self-renewal and stemness and in driving oxidative resistance, including ferroptosis resistance, in LGR4/HOXA9-dependent AML. Understanding the mechanisms by which *GADD45A* manipulates iron-dependent ROS accumulation provides additional insights on ferroptosis regulation and unlocks new arsenal to reverse resistance by restoring the *GADD45A* activity in combination with ferroptosis induction or chemotherapy for treating this poor prognosis subset of leukemia lacking *GADD45A*.

## Acknowledgements

This work was supported by a grant from The Leukemia & Lymphoma Society TRP-23664-23, Cancer Council NSW RG 22-06, Anthony Rothe Memorial Trust Project Grant RRE/0700:sz, and the Tour de Cure Senior Research Grants RSP-187-2020 (to J.Y.W.). We thank Irmela Jeremias and Karsten Spiekermann for providing AML patient-derived xenograft cells; Basit Salik, Karthik B. Polpaya, Gargi A. Kulkarni, Jayvee Datuin, Sheng XF Chen, Jonason Yang, Sayali Gore, and the staff from the UNSW Ramaciotti Centre for Genomics for technical assistance, and the Sydney Children's Tumor Bank Network for providing primary patient samples and related clinical information for this study.

## Authorship Contributions

N.H. and B.M. performed drug treatment and ferroptosis-related experiments with input from X.D.Z., T.L. and J.W.; H.Y. performed murine model experiments; J.S., A.B., N.H. carried out single-cell experiments with input from D.R.C.; L.G. analyzed CITE-seq data with assistance from J.S. and T.C; A.D. performed *in vivo* bioluminescence imaging; S.E.S., D.A.C., R.J.D., D.A.L. supplied mouse *Gadd45a*<sup>-/-</sup> BM cells and provided input on murine model experiments; R.J.D, D.A.L., S.E.S., D.A.C, J.W., G.M.M., M.N., M.H., M.K., B.B.C. reviewed the manuscript; J.Y.W. conceived, designed and analyzed the study and wrote the manuscript.

**Disclosures of Conflict of Interest:** The authors declare no potential conflicts of interest.



## References

1. Krivtsov, A.V., *et al.* Transformation from committed progenitor to leukaemia stem cell initiated by MLL-AF9. *Nature* 442, 818-822 (2006).
2. Stavropoulou, V., *et al.* MLL-AF9 expression in hematopoietic stem cells drives a highly invasive AML expressing EMT-related genes linked to poor outcome. *Cancer cell* 30, 43-58 (2016).
3. George, J., *et al.* Leukaemia cell of origin identified by chromatin landscape of bulk tumour cells. *Nat Commun* 7, 12166 (2016).
4. Shlush, L.I., *et al.* Identification of pre-leukaemic haematopoietic stem cells in acute leukaemia. *Nature* 506, 328-333 (2014).
5. Salik, B., *et al.* Targeting RSPO3-LGR4 Signaling for Leukemia Stem Cell Eradication in Acute Myeloid Leukemia. *Cancer cell* 38, 263-278 (2020).
6. Lynch, J.R., *et al.* Gαq signaling is required for the maintenance of MLL-AF9-induced acute myeloid leukemia. *Leukemia* 30, 1745-1748 (2016).
7. Lynch, J.R. & Wang, J.Y. G protein-coupled receptor signaling in stem cells and cancer. *Int J Mol Sci* 17, 707 (2016).
8. Dietrich, P.A., *et al.* GPR84 sustains aberrant beta-catenin signaling in leukemic stem cells for maintenance of MLL leukemogenesis. *Blood* 124, 3284-3294 (2014).
9. Lynch, J.R., *et al.* JMJD1C-mediated metabolic dysregulation contributes to HOXA9-dependent leukemogenesis. *Leukemia* 33, 1400-1410 (2019).
10. Wang, Y., *et al.* The Wnt/beta-catenin pathway is required for the development of leukemia stem cells in AML. *Science* 327, 1650-1653 (2010).
11. van Rhenen, A., *et al.* High stem cell frequency in acute myeloid leukemia at diagnosis predicts high minimal residual disease and poor survival. *Clin Cancer Res* 11, 6520-6527 (2005).
12. Gentles, A.J., Plevritis, S.K., Majeti, R. & Alizadeh, A.A. Association of a leukemic stem cell gene expression signature with clinical outcomes in acute myeloid leukemia. *JAMA* 304, 2706-2715 (2010).
13. Hollander, M.C., *et al.* Genomic instability in Gadd45a-deficient mice. *Nat Genet* 23, 176-184 (1999).
14. Chen, Y., *et al.* Gadd45a regulates hematopoietic stem cell stress responses in mice. *Blood* 123, 851-862 (2014).
15. Dixon, S.J., *et al.* Ferroptosis: an iron-dependent form of nonapoptotic cell death. *Cell* 149, 1060-1072 (2012).
16. Perugini, M., *et al.* GADD45A methylation predicts poor overall survival in acute myeloid leukemia and is associated with IDH1/2 and DNMT3A mutations. *Leukemia* 27, 1588-1592 (2013).
17. Perugini, M., *et al.* Repression of Gadd45alpha by activated FLT3 and GM-CSF receptor mutants contributes to growth, survival and blocked differentiation. *Leukemia* 23, 729-738 (2009).
18. Wingert, S., *et al.* DNA-damage response gene GADD45A induces differentiation in hematopoietic stem cells without inhibiting cell cycle or survival. *Stem Cells* 34, 699-710 (2016).
19. Gupta, M., Gupta, S.K., Hoffman, B. & Liebermann, D.A. Gadd45a and Gadd45b protect hematopoietic cells from UV-induced apoptosis via distinct signaling pathways, including p38 activation and JNK inhibition. *J Biol Chem* 281, 17552-17558 (2006).
20. Gonzales-Aloy, E., *et al.* miR-101 suppresses the development of MLL-rearranged acute myeloid leukemia. *Haematologica* 104, e296-e299 (2019).
21. Hildesheim, J., *et al.* Gadd45a regulates matrix metalloproteinases by suppressing DeltaNp63alpha and beta-catenin via p38 MAP kinase and APC complex activation. *Oncogene* 23, 1829-1837 (2004).
22. Bagger, F.O., *et al.* BloodSpot: a database of gene expression profiles and transcriptional programs for healthy and malignant haematopoiesis. *Nucleic Acids Res* 44, D917-924 (2016).
23. Kornblau, S.M., *et al.* Highly phosphorylated FOXO3A is an adverse prognostic factor in acute myeloid leukemia. *Clin Cancer Res* 16, 1865-1874 (2010).

24. Shah, N., *et al.* Roles of ChIR1 DNA helicase in replication recovery from DNA damage. *Exp Cell Res* 319, 2244-2253 (2013).
25. Trowbridge, J.J., *et al.* Haploinsufficiency of Dnmt1 impairs leukemia stem cell function through derepression of bivalent chromatin domains. *Genes Dev* 26, 344-349 (2012).
26. Lagadinou, E.D., *et al.* BCL-2 inhibition targets oxidative phosphorylation and selectively eradicates quiescent human leukemia stem cells. *Cell stem cell* 12, 329-341 (2013).
27. Stuart, T., *et al.* Comprehensive Integration of Single-Cell Data. *Cell* 177, 1888-1902 e1821 (2019).
28. Goardon, N., *et al.* Coexistence of LMPP-like and GMP-like leukemia stem cells in acute myeloid leukemia. *Cancer cell* 19, 138-152 (2011).
29. Xie, Y., Kuang, F., Liu, J., Tang, D. & Kang, R. DUSP1 blocks autophagy-dependent ferroptosis in pancreatic cancer. *J. Pancreatol.* 3, 154-160 (2020).
30. Kesarwani, M., *et al.* Targeting c-FOS and DUSP1 abrogates intrinsic resistance to tyrosine-kinase inhibitor therapy in BCR-ABL-induced leukemia. *Nat Med* 23, 472-482 (2017).
31. Honarmand Ebrahimi, K., Hagedoorn, P.L. & Hagen, W.R. Unity in the biochemistry of the iron-storage proteins ferritin and bacterioferritin. *Chem Rev* 115, 295-326 (2015).
32. Muckenthaler, M.U., Rivella, S., Hentze, M.W. & Galy, B. A Red Carpet for Iron Metabolism. *Cell* 168, 344-361 (2017).
33. Toulabi, K., *et al.* Physical and functional cooperation between AP-1 and beta-catenin for the regulation of TCF-dependent genes. *Oncogene* 26, 3492-3502 (2007).
34. Jang, H.H., *et al.* Two enzymes in one; two yeast peroxiredoxins display oxidative stress-dependent switching from a peroxidase to a molecular chaperone function. *Cell* 117, 625-635 (2004).
35. Kanwal, R., *et al.* Protection against oxidative DNA damage and stress in human prostate by glutathione S-transferase P1. *Mol Carcinog* 53, 8-18 (2014).
36. Bertoli, S., *et al.* Ferritin heavy/light chain (FTH1/FTL) expression, serum ferritin levels, and their functional as well as prognostic roles in acute myeloid leukemia. *Eur J Haematol* 102, 131-142 (2019).
37. Yang, W.S., *et al.* Regulation of ferroptotic cancer cell death by GPX4. *Cell* 156, 317-331 (2014).
38. Rogakou, E.P., Nieves-Neira, W., Boon, C., Pommier, Y. & Bonner, W.M. Initiation of DNA fragmentation during apoptosis induces phosphorylation of H2AX histone at serine 139. *J Biol Chem* 275, 9390-9395 (2000).
39. Olive, P.L. & Banath, J.P. The comet assay: a method to measure DNA damage in individual cells. *Nat Protoc* 1, 23-29 (2006).
40. Krivtsov, A.V., *et al.* Cell of origin determines clinically relevant subtypes of MLL-rearranged AML. *Leukemia* 27, 852-860 (2013).
41. Ito, K., *et al.* Reactive oxygen species act through p38 MAPK to limit the lifespan of hematopoietic stem cells. *Nat Med* 12, 446-451 (2006).
42. Santos, M.A., *et al.* DNA-damage-induced differentiation of leukaemic cells as an anti-cancer barrier. *Nature* 514, 107-111 (2014).
43. Kang, M.A., So, E.Y., Simons, A.L., Spitz, D.R. & Ouchi, T. DNA damage induces reactive oxygen species generation through the H2AX-Nox1/Rac1 pathway. *Cell Death Dis* 3, e249 (2012).
44. Tadokoro, T., *et al.* Mitochondria-dependent ferroptosis plays a pivotal role in doxorubicin cardiotoxicity. *JCI Insight* 5, e132747 (2020).
45. Kietzmann, T., Petry, A., Shvetsova, A., Gerhold, J.M. & Gorch, A. The epigenetic landscape related to reactive oxygen species formation in the cardiovascular system. *Br J Pharmacol* 174, 1533-1554 (2017).
46. Tsai, H.C., *et al.* Transient low doses of DNA-demethylating agents exert durable antitumor effects on hematological and epithelial tumor cells. *Cancer cell* 21, 430-446 (2012).
47. Cancer Genome Atlas Research, N. Genomic and epigenomic landscapes of adult de novo acute myeloid leukemia. *N Engl J Med* 368, 2059-2074 (2013).

## Figure Legends

### Figure 1. *Gadd45a* is negatively regulated by *Lgr4* and its deletion retains $\beta$ -catenin activity even in the absence of *Lgr4*.

- (A) Heat map analysis of microarray data (n=3,  $p \leq 0.005$ , fold change  $\geq 1.8$ ) showing differentially expressed genes induced by *Lgr4* knockdown in MLL-AF9-induced AML cells.
- (B) qPCR (n=3) and western blots confirming upregulation of *Gadd45a* induced by *Lgr4* knockdown in MLL-AF9 leukemic cells carrying scrambled control (Scr) versus *Lgr4* shRNA1 (sh1). Mean  $\pm$  SD. \* $p < 0.05$ , unpaired t-test.
- (C) qPCR (n=3) and western blots showing downregulation of *Gadd45a* induced by *Lgr4* overexpression in HOXA9/MEIS1 leukemic cells, compared with endogenous expression of *Gadd45a* in MLL-AF9 leukemic cells. Mean  $\pm$  SD. \*\*\*\* $p < 0.0001$ , one-way ANOVA.
- (D) Analysis of the TCGA dataset<sup>22,47</sup> revealing the correlation between *LGR4* and *GADD45A* expression in all AML patients (n=244,  $r = -0.328$ ,  $p = 1.6e-07$ ), AML patients with unfavorable outcome (n=81,  $r = -0.482$ ,  $p = 5.1e-06$ ), and AML patients with favorable outcome (n=120,  $r = -0.155$ ,  $p = 0.091$ ).
- (E) Western blots confirming efficient *Gadd45a* knockout with a resultant increase in  $\beta$ -catenin and inactive phospho-Ser9-Gsk3 $\beta$  (p-Gsk3 $\beta$ <sup>Ser9</sup>) in GFP<sup>+</sup> pre-MLL<sup>c-Kit+</sup> cells. qPCR showing upregulation of Wnt/self-renewal target genes induced by *Gadd45a* deletion (n=3). Mean  $\pm$  SD. \* $p < 0.05$ , \*\* $p < 0.005$ , unpaired t-test.
- (F) Colony-formation of *Gadd45a*<sup>-/-</sup> versus *Gadd45a*<sup>+/+</sup> pre-MLL<sup>c-Kit+</sup> cells. The percentage of colonies (relative to *Gadd45a*<sup>-/-</sup>) at the 3rd round of serial replating is shown. n=4 independent experiments. Mean  $\pm$  SD. \*\* $p < 0.005$ , unpaired t-test.
- (G) Western blots confirming efficient *Lgr4* knockdown with a resultant change of endogenous  $\beta$ -catenin expression in response to *Gadd45a* knockout in LSCs (Lin<sup>-</sup>Sca-1<sup>c</sup>Kit<sup>high</sup>CD16/32<sup>high</sup>CD34<sup>+</sup>), flow-sorted from the BM of AML mice following transplantation with pre-MLL<sup>c-Kit+</sup> cells.

**Figure 2. Deletion of *Gadd45a* enhances oncogenic potential and LSC activity upon serial transplantation while inducing mutations.**

(A) Schematic overview of the experimental procedure.

(B-E) Kaplan-Meier mouse survival curves of primary AML (B), secondary AML (C), tertiary AML (D) and quaternary AML (E). Primary AML was generated by transplanting  $1 \times 10^6$  *Gadd45a*<sup>-/-</sup> versus *Gadd45a*<sup>+/+</sup> pre-leukemic cells, induced by MLL-AF9-GFP, into sublethally irradiated BL6 recipient mice (n=6 for each group). Secondary AML, tertiary AML and quaternary AML were generated by transplanting  $1 \times 10^4$  GFP<sup>+</sup> leukemic BM cells flow-sorted from mice with primary, secondary and tertiary AML, respectively into recipient mice (n=6 for each group). *P* was determined by the log-rank test.

(F) *In vivo* limiting dilution transplantation assay showing a 10-fold increase in LSC frequency in *Gadd45a*<sup>-/-</sup> versus *Gadd45a*<sup>+/+</sup> mice (1/142 versus 1/1650, *p*=0.00114). LSC frequency was calculated using L-Calc<sup>TM</sup> software (StemCell Technologies). Kaplan-Meier survival curves of mice receiving the indicated number of GFP<sup>+</sup> leukemic BM cells (n=6 for each group), and *P* was determined by the log-rank test.

(G) Scatter plots with a bar graph depicting the percentage of Gr-1<sup>-low</sup>c-Kit<sup>high</sup> population in total GFP<sup>+</sup> leukemic BM cells from *Gadd45a*<sup>-/-</sup> versus *Gadd45a*<sup>+/+</sup> mice (n=5 for each group). Mean  $\pm$  SD. \*\*\**p* < 0.0005. Unpaired t-test.

(H) Stacked bar plots displaying the number of coding mutations identified by whole-genome sequencing (WGS) of *Gadd45a*<sup>-/-</sup> versus *Gadd45a*<sup>+/+</sup> LSCs from primary (1<sup>st</sup>) and tertiary (3<sup>rd</sup>) AML. Green, yellow and silver stacked bars represent synonymous, missense, and others (inframe insertion/deletion, frameshit, splice donor variant in coding sequence, start lost and stop retained/gained), respectively.

(I) Distribution of the coding mutations in *Gadd45a*<sup>-/-</sup> versus *Gadd45a*<sup>+/+</sup> LSCs from primary AML.

(J) Flow cytometry histograms showing decreased intracellular ROS in *Gadd45a*<sup>-/-</sup> LSCs compared with *Gadd45a*<sup>+/+</sup> LSCs.

(K) The number of colonies following treatment of *Gadd45a*<sup>-/-</sup> versus *Gadd45a*<sup>+/+</sup> AML LSCs with DMSO control or doxorubicin (DOX: 2.5 ng/mL or 5 ng/mL) for 5 days in methylcellulose (n=4). Mean  $\pm$  SD. \**p* < 0.05, \*\**p* < 0.005, \*\*\**p* < 0.0005; NS, not significant (*p* > 0.05). One-way ANOVA.

(L) *In vivo* BrdU proliferation assay with dot plots depicting BrdU<sup>+</sup> GFP<sup>+</sup> leukemic cells engrafted in the mouse BM at 12 days post-transplantation. *Gadd45a*<sup>-/-</sup> or *Gadd45a*<sup>+/+</sup> AML LSCs were pre-treated *ex vivo* with DMSO versus 5 ng/mL DOX for 48 hours and  $1 \times 10^5$  treated cells were transplanted into BL6 mice for leukemic cell engraftment and subsequent BrdU proliferation assay. Data are presented as the mean percentage relative to DMSO  $\pm$  SD (n=5 mice per group). \*\*\**p* < 0.0001; NS, not significant (*p* > 0.05). Unpaired t-test.

(M) Flow cytometry histograms showing intracellular ROS levels in *Gadd45a*<sup>-/-</sup> versus *Gadd45a*<sup>+/+</sup> AML LSCs treated with DMSO versus DOX (2.5 ng/mL or 5 ng/mL) for 5 days, or pre-treated with 1 mM N-acetylcysteine (NAC) for 1 hour followed by treatment with 100  $\mu$ M menadione for an additional 1 hour.

**Figure 3. Deletion of *GADD45A* promotes engraftment of human AML PDX cells in NSG mice.**

(A) Schematic describing *in vivo* generation of CRISPR/Cas9-mediated knockout (KO) of *GADD45A* in PDX mice. Also see **Supplemental Figure 4** for the additional experimental detail.

(B) Representative *in vivo* bioluminescence imaging and total flux (photons/sec; p/s) of *GADD45A* KO PDX mice (n=9) versus CRISPR control (Ctr) PDX mice (n=6) in primary NSG recipients.  $5 \times 10^4$  mCherry<sup>+</sup> GFP<sup>+</sup> PDX cells were transplanted into each of recipient mice. Scatter dot plots represent the mean  $\pm$  SD. \*\*\*p < 0.0005, \*\*\*\*p < 0.0001, two-way ANOVA.

(C) Representative *in vivo* bioluminescence imaging and total flux (p/s) of *GADD45A* KO PDX mice (n=5) versus CRISPR Ctr PDX mice (n=6) in secondary NSG recipients.  $1 \times 10^5$  mCherry<sup>+</sup> PDX cells from primary recipient mice were transplanted into each of secondary recipient mice. Mean  $\pm$  SD. \*\*p < 0.005, \*\*\*p < 0.0005, \*\*\*\*p < 0.0001, two-way ANOVA.

(D) qPCR confirming stable knockout of *GADD45A* and showing relative expression levels of WNT/self-renewal target genes in *GADD45A* KO versus CRISPR Ctr hCD33<sup>+</sup> PDX BM cells (n=3). Mean  $\pm$  SEM. \*p < 0.05, \*\*p < 0.005, unpaired t-test.

**Figure 4. Coupling scRNA-seq with CITE-seq on AML PDX cells reveals an increased proportion of LSCs and identifies genes/pathways upregulated by *GADD45A* deletion at a single stem cell level.**

(A) t-SNE clustering of CITE-seq data showing human CD34<sup>+</sup> LSC-enriched subpopulations (in red) with *GADD45A* KO (n=1,511 cells, 19.6%) versus CRISPR Ctr (n=542 cells, 8.7%) in the BM of PDX mice. Cutoff: min = q85 and max = q97 (q stands for quantile).

(B) Heatmap of integrated CITE-seq data analysis identifying 43 differentially expressed genes (DEGs) upregulated in *GADD45A* KO PDX LSCs (n=233 cells), compared with CRISPR Ctr LSCs (n=110 cells). The LSC compartment (CD34<sup>+</sup>CD38<sup>-</sup>CD45RA<sup>+</sup>CD90<sup>-</sup>) was defined by a stringent cutoff of CD34 > q85, CD38 < q50, CD45RA > q65, CD90 < q65. Wilcoxon rank-sum test, fold-change > 1.4 and adjusted p-value with Benjamini-Hochberg method < 0.05.

(C) Bar chart showing the top 9 enriched cancer-associated pathways from MSigDB oncogenic signatures, along with their corresponding p-values and associated DEGs.

(D) Scatter plot showing GO function enrichments of the DEGs upregulated in *GADD45A* KO LSCs, compared with CRISPR Ctr LSCs. Clusters were computed using the Leiden algorithm and similar gene sets were clustered together. Larger, black-outlined points represent significantly enriched terms. Points are plotted on the first two UMAP dimensions. The table lists enriched gene sets with p < 8.0e-04 and associated DEGs.

(E) Fast pre-ranked GSEA (FGSEA) of CITE-seq data (cutoff: padj < 0.05 and NES > 1.8) identifying *GADD45A* loss-induced enrichment of gene sets associated with ROS sensing by NFE2L2, detoxification of ROS, cellular response to chemical stress, and iron uptake and transport, upon *GADD45A* knockout in human AML PDX cells.

(F) Kaplan-Meier curves of overall survival for 172 AML patients, as stratified by expression levels of *FTH1* (p=0.0039) and *PRDX1* (p=0.019) in the TCGA dataset.

**Figure 5. Deletion of *GADD45A* prevents RSL3-induced ferroptosis and DNA damage through upregulation of FTH1.**

(A) Flow cytometry dot plots showing the percentage of nonapoptotic or ferroptotic cell death (Annexin V-negative, SYTOX Blue-positive; Q3), following treatment of *Gadd45a*<sup>-/-</sup> versus *Gadd45a*<sup>+/+</sup> AML LSCs with DMSO or 3  $\mu$ M RSL3 for 4 days in methylcellulose.

(B) Percentages of viable cells measured by trypan blue exclusion assay in *Gadd45a*<sup>-/-</sup> versus *Gadd45a*<sup>+/+</sup> LSCs, following treatment with DMSO or 3  $\mu$ M RSL3 for 4 days in methylcellulose (n=3). Mean  $\pm$  SD. \*\*p < 0.005; NS, not significant (p > 0.05). Unpaired t-test.

(C) *In vivo* BrdU proliferation assay with dot plots showing the percentage of BrdU<sup>+</sup>DAPI<sup>+</sup> leukemic cells engrafted in the mouse BM at 21 days post-transplantation. *Gadd45a*<sup>-/-</sup> versus *Gadd45a*<sup>+/+</sup> LSCs were pre-treated *ex vivo* with DMSO or 3  $\mu$ M RSL3 for 4 days in methylcellulose and 1 $\times$ 10<sup>5</sup> GFP<sup>+</sup> treated cells were then transplanted into BL6 mice for the engraftment of GFP<sup>+</sup> LSCs and subsequent *in vivo* BrdU cell proliferation assay. Data are presented as the mean percentage relative to DMSO  $\pm$  SD.

\*\*\*p < 0.0005; NS, not significant (p > 0.05). Unpaired t-test.

(D) qPCR (n=3) showing upregulation of *Gadd45a* and downregulation of *Fth1* induced by RSL3 treatment in *Gadd45a*<sup>+/+</sup> LSCs but not in *Gadd45a*<sup>-/-</sup> LSCs. Mean  $\pm$  SD. \*\*p < 0.005; NS, not significant (p > 0.05), unpaired t-test.

(E) qPCR (n=3) confirming efficient knockdown of *Fth1* by shRNA (*Fth1*-sh) in *Gadd45a*<sup>-/-</sup> LSCs and *Gadd45a*<sup>+/+</sup> LSCs. Mean  $\pm$  SD. \*p < 0.05, \*\*\*\*p < 0.0001, unpaired t-test.

(F) Flow cytometry histograms illustrating intracellular iron (Fe<sup>2+</sup>) and ROS levels in *Gadd45a*<sup>-/-</sup> versus *Gadd45a*<sup>+/+</sup> LSCs carrying Scr or *Fth1*-sh, following treatment with DMSO or 3  $\mu$ M RSL3 for 4 days in methylcellulose.

(G) Percentages of viable cells measured by trypan blue exclusion assay in *Gadd45a*<sup>-/-</sup> versus *Gadd45a*<sup>+/+</sup> LSCs carrying Scr or *Fth1*-sh, following treatment with DMSO or 3  $\mu$ M RSL3 for 4 days in methylcellulose (n=3). Mean  $\pm$  SD. \*\*p < 0.005, \*\*\*\*p < 0.0001; NS, not significant (p > 0.05). One-way ANOVA.

(H) Western blots showing increased expression of  $\gamma$ H2AX induced by RSL3 treatment in *Gadd45a*<sup>+/+</sup> LSCs but not in *Gadd45a*<sup>-/-</sup> LSCs.

(I) Alkaline comet assay used to quantify the level of DNA-strand breaks illustrating heightened DNA damage (tail moment) in *Gadd45a*<sup>+/+</sup> LSCs treated in methylcellulose with 3  $\mu$ M RSL3 compared to DMSO. Scatter plots with a bar graph depicting tail moments (a combined measure of tail length and the amount of migrated DNA) calculated using CometScore. Representative fluorescence images showing DAPI-stained single cells after electrophoresis (20x magnification). During electrophoresis, damaged DNA migrated out of the nucleus toward the anode forming a comet tail, while undamaged DNA remained in the comet head. The comet tail moment represents the extent of DNA damage in individual cells.

**Figure 6. Lack of *GADD45A* influences the response of primary human AML cells to ferroptosis induction.**

(A) Percentages of viable cells (DAPI-negative) in *GADD45A*-KO versus CRISPR-Ctr mCherry<sup>+</sup> human AML PDX cells, following *ex vivo* treatment with 3  $\mu$ M RSL3 for 24 hours. n=3 independent experiments. Mean  $\pm$  SD. \*p < 0.05, \*\*\*p < 0.0005, unpaired t-test.

(B) Percentages of viable (DAPI-negative) mCherry<sup>+</sup> human AML cells (n=3, mean  $\pm$  SD) and qPCR of *GADD45A* expression (n=6, mean  $\pm$  SEM) in CRISPR-Ctr PDX BM cells, pre-treated *ex vivo* for 18 hours with 5  $\mu$ M Fer-1 (ferroptosis inhibitor) and subsequently treated with 3  $\mu$ M RSL3 (ferroptosis inducer) for an additional 24 hours. \*p < 0.05, \*\*\*\*p < 0.0001; NS, not significant (p > 0.05). One-way ANOVA.

(C) qPCR showing relative expression levels of *GADD45A* in primary specimens from AML patients (n=6), compared with remission samples (n=2). Mean  $\pm$  SD. n=3 replicates. \*\*\*p < 0.0005, \*\*\*\*p < 0.0001, one-way ANOVA. *Note*: Two paired diagnostic/remission samples: AML-NK\_1/remission\_1 and AML-NK\_2/remission\_2, showing higher levels of *GADD45A* at remission than paired diagnosis, consistent with higher expression of *GADD45A* in normal human BM and CD34<sup>+</sup> cells than in MLL-rearranged AML patients (**Supplemental Figure 8**).

(D) Schematic overview of AML patient specimens responding to ferroptosis inducers RSL3 *ex vivo*.

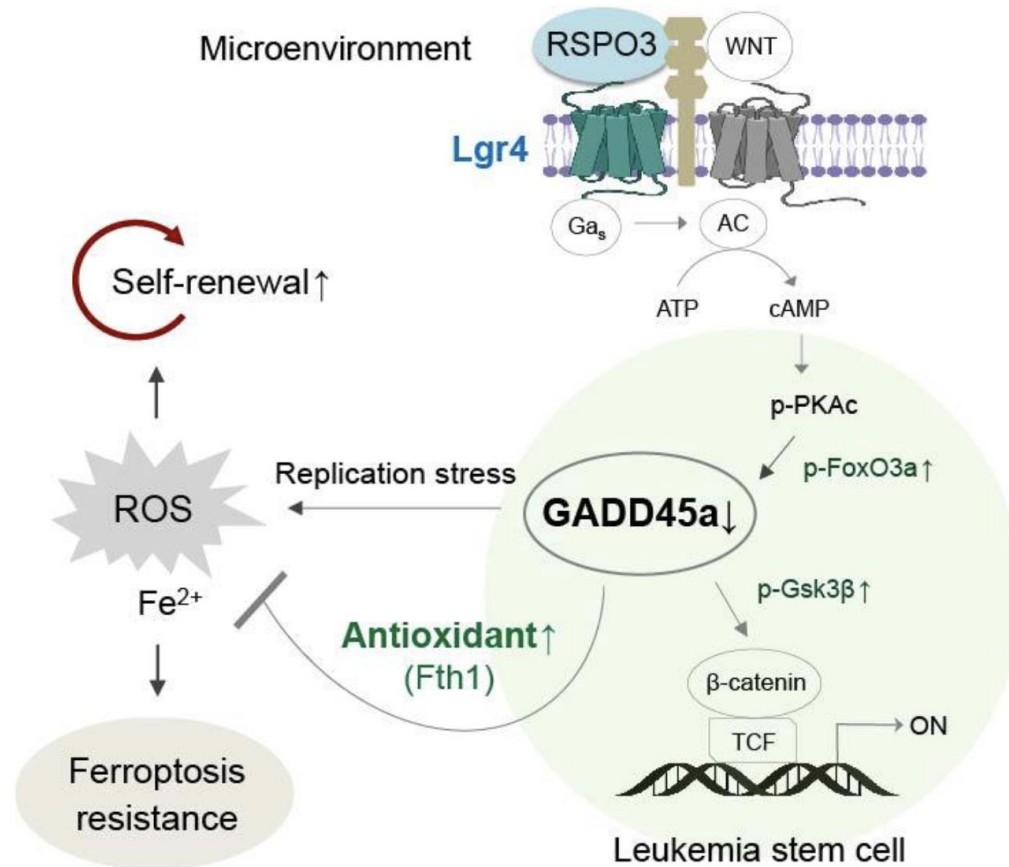
(E) Intracellular ferrous iron (Fe<sup>2+</sup>) was detected using the fluorescent turn-off sensor Phén Green (PG) SK that is quenched upon binding iron, while ROS levels were measured using the lipid peroxidation sensor C11-BODIPY (581/591) that shifts its fluorescence from red (~590 nm) to green (~530 nm) upon oxidation in hCD34<sup>+</sup> primary AML patient specimens, following *ex vivo* treatment with 3  $\mu$ M RSL3 for 24 hours.  $\Delta$ PG-SK revealed the reversed value of PG-SK fluorescence quenching, showing an increased intracellular Fe<sup>2+</sup> in hCD34<sup>+</sup> cells from an AML patient with APL but not 9p deletion. Mean  $\pm$  SD. \*\*p < 0.005, \*\*\*p < 0.0005; NS, not significant (p > 0.05). Unpaired t-test. Also see **Supplemental Figure 9** for additional patient samples examined.

(F) Percentages of viable cells (n=4 replicates, mean  $\pm$  SD) tested using the alamarBlue assay in primary AML patient specimens pre-treated *ex vivo* for 18 hours with 5  $\mu$ M Fer-1, followed by treatment with 3  $\mu$ M RSL3 for an additional 24 hours. \*\*\*p < 0.0005, \*\*\*\*p < 0.0001; NS, not significant (p > 0.05). One-way ANOVA.

(G) qPCR of *GADD45A* expression (mean  $\pm$  SEM) in primary AML patient specimens pre-treated *ex vivo* for 18 hours with 5  $\mu$ M Fer-1, followed by treatment with 3  $\mu$ M RSL3 for an additional 24 hours. \*\*\*p < 0.0005; NS, not significant (p > 0.05). One-way ANOVA.



# Linking Loss of the Stress Sensor GADD45A to Stemness and Ferroptosis Resistance in Acute Myeloid Leukemia (AML)



Partially created  
with Biorender.com

**Conclusions:** GADD45A loss regulates ferroptosis resistance and leukemia stem cell activity through the upregulation of antioxidant FTH1, which sustains low-ROS for maintaining self-renewal and preventing ferroptosis in AML.

Hassan et al. DOI: 10.xxxx/*blood*.2024xxxxxx.

**Blood  
Visual  
Abstract**